Technical note: a novel servo-driven dual-roller handrim wheelchair ergometer

De Klerk, R.; Vegter, R. J.K.; Veeger, DirkJan; van der Woude, L.H.V.

DOI
10.1109/TNSRE.2020.2965281

Publication date
2020

Document Version
Final published version

Published in
IEEE Transactions on Neural Systems and Rehabilitation Engineering

Technical Note: A Novel Servo-Driven Dual-Roller Handrim Wheelchair Ergometer

R. de Klerk, R. J. K. Vegter, H. E. J. Veeger, and L. H. V. van der Woude

***Abstract*— The measurement of handrim wheelchair propulsion characteristics and performance in the field is complicated due to the non-stationary nature of wheelchair driving. In contrast, the laboratory provides a constrained and standardisable environment to conduct measurements and experiments. Apart from wheelchair treadmills, dynamometers or ergometers for handrim wheelchairs are often custom-made, one-of-a-kind, expensive, and sparsely documented in the research literature. To facilitate standardised and comparable lab-based measurements in research, as well as in clinical settings and adapted sports, a new wheelchair ergometer was developed. The ergometer with instrumented dual rollers allows for the performance analysis of individuals in their personal handrim wheelchair and facilitates capacity assessment, training and skill acquisition in rehabilitation or adapted sports. The ergometer contains two servomotors, one for each rear wheel roller, that allow for the simulation of translational inertia and resistive forces as encountered during wheelchair propulsion based on force input and a simple mechanical model of wheelchair propulsion. A load cell configuration for left and right roller enables the measurement of effective user-generated torque and force on the handrim and the concomitant timing patterns. Preliminary results are discussed.**

***Index Terms*— Dynamometer, ergometry, biomechanics, power output, wheelchair training.**

I. Introduction

HANDRIM wheelchair propulsion is characterized as a straining and inefficient activity that produces high repetitive strain on the upper extremities, resulting in an increased risk of musculoskeletal problems [1], [2] and/or inactive lifestyle [3]. To improve physical capacity, wheelchair technology, individual propulsion technique, wheelchair propulsion biomechanics has been extensively studied [4]–[7]. Oftentimes studies use a combination of physiological, kinematic, and kinetic outcomes, requiring highly specialized equipment. Research is generally conducted on systems that simulate (to some extent) overground wheelchair propulsion, such as dynamometers, ergometers, or treadmills as they allow for measurements and training interventions to be performed in a controlled environment.

The validity of these lab-based experiments relies not only on the instrumentation and its measurement capabilities, but also on the simulation quality that these systems provide [8]. In addition to allowing for valid and reliable measurements of power output on the wheels, a simulator should provide an adequate simulation of the frictional losses, environmental conditions, and inertia of the wheelchair-user system. Finally, this should all be possible without altering the existing wheelchair-user interface [9] while facilitating other measurements such as metabolic cost, kinematics or electromyography.

Wheelchair propulsion on a motorized treadmill is probably the most realistic way of simulating wheelchair propulsion in the lab, but also has a number of drawbacks. On a treadmill the frictional forces and inertia are comparable to overground propulsion [10], while steering as well as visual position control are a necessity [11]. However, air resistance is absent, which becomes an important resistive force at speeds beyond 2m/s [12], [13]. Although a standardised drag test can determine average power output without altering the wheelchair-user interface [14], [15], it conveys no information about propulsion technique. Additionally, a treadmill mostly does not allow for sprinting or acceleration tasks to be performed and athletes can often exceed the maximum treadmill speed [16]. Other than that, treadmills can be too narrow and some labs and/or manufacturers therefore require a sidebar connected to the wheelchair to secure the stability of the wheelchair on the treadmill [17], which in turn could impact testing validity.

To cope with the aforementioned problems, a variety of different ergometers have been developed in the past [18]. Some are purely mechanical and others have electrical components to simulate overground propulsion mechanics. Inertia is generally simulated with a fixed-sized flywheel or weighted rollers and cannot be adjusted to an individual wheelchair-user combination. Few systems allow for the determination of push technique or even power output. Finally, they are often highly

Manuscript received July 13, 2019; revised November 13, 2019; accepted November 25, 2019. Date of publication February 11, 2020; date of current version April 8, 2020. This work was supported in part by the Grant from Samenwerkingsverband Noord-Nederland under Grant OPSNN0109 and in part by the PPP-Allowance of the Top Consortia for Knowledge and Innovation of the Ministry of Economic Affairs. *(Corresponding author: R. De Klerk.)*

R. de Klerk and R. J. K. Vegter are with the Center for Human Movement Sciences, University Medical Centre Groningen, University of Groningen, 9713 AV Groningen, The Netherlands (e-mail: r.de.klerk@umcg.nl; r.j.k.vegter@umcg.nl).

H. E. J. Veeger is with the Department of Human Movement Sciences, Institute for Fundamental and Clinical Human Movement Sciences, Vrije Universiteit Amsterdam, 1081 BT Amsterdam, The Netherlands, and also with the Man-Machine Systems and Control Group, Department of Mechanical Engineering, Delft University of Technology, 2600 AA Delft, The Netherlands (e-mail: h.e.j.veeger@vu.nl).

L. H. V. van der Woude is with the Center for Human Movement Sciences, University Medical Centre Groningen, 9713 AV Groningen, The Netherlands, and also with the Centre for Rehabilitation, University Medical Centre Groningen, 9713 AV Groningen, The Netherlands (e-mail: l.h.v.van.der.woude@umcg.nl).

Digital Object Identifier 10.1109/TNSRE.2020.2965281

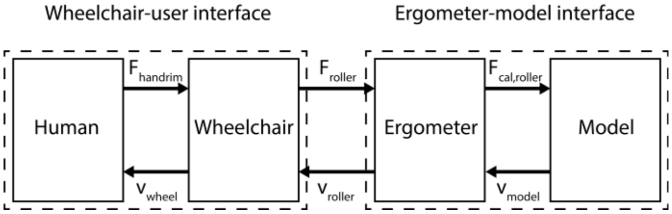

Fig. 1. Schematic overview of ergometer feedback control scheme [38].

specialized pieces of equipment [8] that can only be operated in a few specialized labs. Widespread implementation of wheelchair biomechanical measurements can only be achieved when an easy-to-use system is available. Such a system should have standardized protocols and produce standardized results. Currently, no such system is available.

In the current paper, a newly developed commercial handrim wheelchair ergometer is presented that aims to provide the researcher, clinician, coach or athlete with a system that allows for accurate measurements for independent left and right-hand propulsion actions during exercise testing or training, while providing a mechanically realistic simulation of overground propulsion without adjusting the wheelchair-user interface. The ergometer includes a real time simulation of wheelchair propulsion based on a simple mechanical model of wheelchair propulsion [8], with user requirement dependent options such as inertia, rolling friction, air friction, and slopes. The system provides feedback on propulsion speed, power output, as well as push characteristics, if need be in a virtual environment. The purpose of this technical note is to provide a thorough description of the ergometer and to demonstrate its functionalities.

II. System Overview

The Esseda is a novel wheelchair ergometer developed and produced by Lode BV (Groningen, The Netherlands) in collaboration with the University of Groningen, University Medical Centre Groningen, (UMCG), Centre for Human Movement Sciences, Groningen, The Netherlands. The ergometer measures the force production of the wheelchair user with a load cell configuration and simulates overground wheelchair propulsion in an admittance-control feedback loop (Fig. 1). In the following sections the ergometer design, the measurement system, simulations, and calibrations will be further discussed.

A. Physical Design

The ergometer (l = 3.01m w = 1.39m) consists of two nearly identical modules; one for the left wheel and one for the right wheel (Fig. 2). Both modules have their own roller (l = 0.43m, d = 0.10m), servomotor, and control unit. The gap between the rollers is 0.36m wide. It includes a ramp (∼10°) to allow wheelchairs to access the ergometer and a front panel to support the castor wheels with an extension for wheelers. A wheelchair can be centred on the rollers with the alignment system. Four tie downs are used to strap the wheelchair to the ergometer.

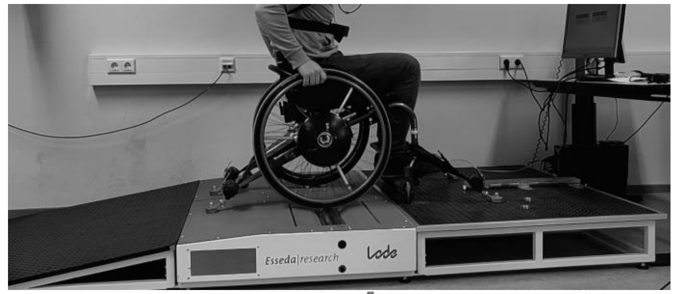

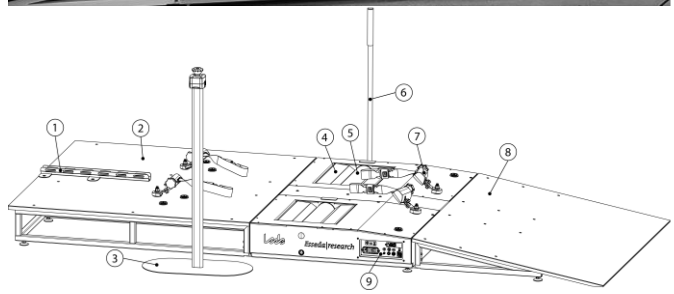

Fig. 2. The Esseda wheelchair ergometer. Bottom: 1. Wheeler extension; 2. Castor support board; 3. Emergency stop; 4: Alignment flaps (4x); 5. Roller (2x); 6: Alignment handle; 7: Straps (4x); 8: Ramp; 9: Communication module.

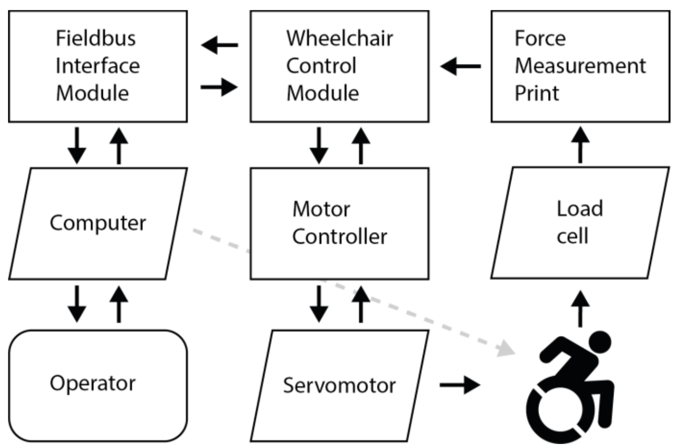

Fig. 3. Overview of the electronics layout for the wheelchair ergometer. The wheelchair control module, motor controller, servomotor, force measurement print, and load cell are present in both sides of the ergometer.

B. Electronics

Most electronic components are designed by Lode BV and custom-made for the ergometer. Both modules contain a loadcell (Utilcell Model 300, 50kg, combined error = 0.017%, creep = 0.016%, temperature drift = 0.02% per 5°K) with a Force Measure Print PCBA (printed circuit board assembly), a wheelchair control module PCBA, and a brushless servomotor (Schneider Electric BMH0703T11F2A, nominal output = 900W, nominal torque = 2.9Nm, peak stall torque = 10.2Nm) with controller (Schneider Electric Lexium 32C). The motor:roller gear ratio is 2:1, resulting in a top speed of 12.5ms^{-1}. The left module also contains the net filter and a communication module (Fieldbus Interface Module) in addition to the previously mentioned electronics. An overview of the electronics setup can be found in Fig. 3. It is possible to send a 24V synchronisation pulse to the ergometer to synchronise data with other measurement devices.

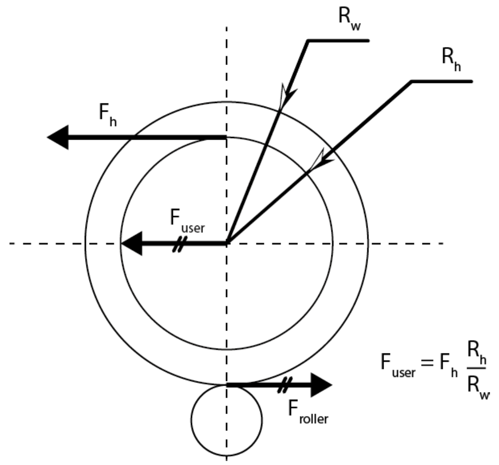

Fig. 4. User generated effective component of the total handrim forces and torques (not shown) are indirectly measured through the roller [4]. This force can be inferred when information about the wheel size and handrim size is available.

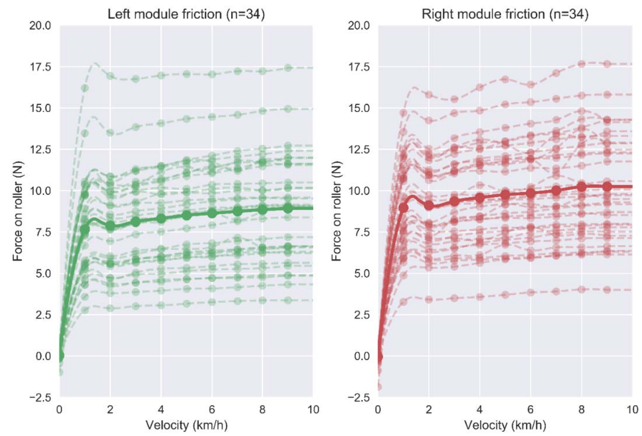

Fig. 5. Individual and mean calibration curves for 34 participants in their personal wheelchair. Every calibration is different due to differences in mass, the distribution thereof, and the tension on the fastening straps. The spline (as shown) was replaced with a linear interpolation (firmware version 1.0.4).

C. Control Software (Firmware)

The ergometer is controlled with closed-source embedded firmware developed and maintained by Lode BV in the C programming language. Calculations in the control loop were verified by researchers at the UMCG. The control loop receives force data, calculates a new control speed, and sends the new control speed to the motor controller at 100Hz [19] in an interrupt-controlled loop. If the firmware receives erroneous values the ergometer automatically stops.

D. Associated Software

The ergometer can be controlled with a (Windows) computer using the proprietary Lode Ergometry Manager (LEM) software. As of yet there is no Application Programming Interface (API) available. Friction and inertia can be set in LEM and they can be adjusted manually during a measurement or by setting a predetermined protocol. Feedback to the participant is also managed through LEM. Currently, LEM only supports showing speed, target speed, and basic heading to the participant. The default interface is a line-plot of left and right velocity with respect to a target line. Participants can infer directionality and speed from this plot in a natural way. Finally, LEM includes an analysis screen for the operator. This screen provides basic feedback on the distance travelled (m), speed (m/s), amount of work performed (J), and power output (W). The current version does not yet provide a detailed push-by-push analysis as used with measurement wheels and previous research ergometers [20]–[22]. A report (.pdf) can be generated with some precalculated common outcome parameters or raw force and velocity data (100Hz) can be exported to a Microsoft Excel (.xls) file to allow for further processing by a researcher with their preferred data processing software (e.g. Python, R, MATLAB).

III. Measurement Principles

The effective component of the user generated force (and torques) exerted in the handrim can be calculated from the force measured at the roller (F_{roller}) when information about the wheel size relative to the handrim size is available (Fig. 4).

However, user force is not the only force acting on the roller. Two additional components need to be considered, namely: the internal friction of the wheelchair-ergometer system ($F_{frict,int}$) and the combined inertia ($F_{inertia,int}$) of the wheelchair wheel (usually unknown constant) and the roller of the ergometer (known constant).

$$F_{user} = F_{roller} = F_{meas} + F_{frict,int} + F_{inertia,int} \quad (1)$$

A. System Friction

System friction is determined and adjusted for with a dynamic calibration [23]. During a dynamic calibration the ergometer samples the measured force from 0 to 2.5 m/s in steps of 0.28 m/s. Finally, a linear interpolation [24] function is used to estimate intermediate values and friction is assumed to be constant above 2.5 m/s. As an indication of friction found in the field: in a recent trial, 34 wheelchair users were measured in their personal everyday wheelchair. All tires were inflated to 6 bars (600kPa) before the measurement. A dynamic calibration was performed with the participant in an upright stationary natural position after the wheelchair had been fastened on the ergometer. The resulting calibration curves are shown in Fig. 5 for the left and the right module respectively. These calibration curves show that individual calibration curves are different for each wheelchair-user combination, in dependence of the wheelchair design/condition, fastening, and total weight, but follow a similar pattern. As such, they highlight the importance of a proper individual calibration before the onset of each measurement to compensate for inter- and intra-individual differences.

B. System Inertia

During dynamic conditions the system inertia of both the wheelchair and ergometer significantly impacts the force readings of the ergometer. The inertia was estimated to be

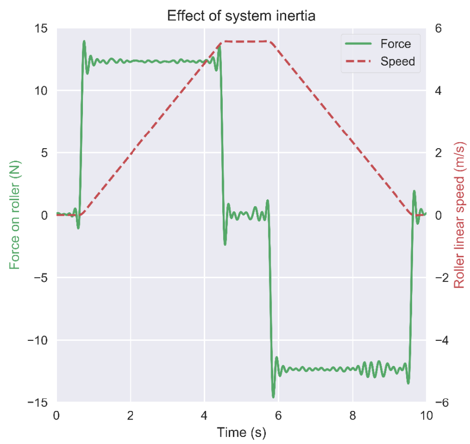

Fig. 6. Single force measurement (5Hz, 2nd order filtered) during acceleration and deceleration of the rollers without a wheelchair after adjusting for system friction. The measured force is acceleration dependent and reflective of the system inertia.

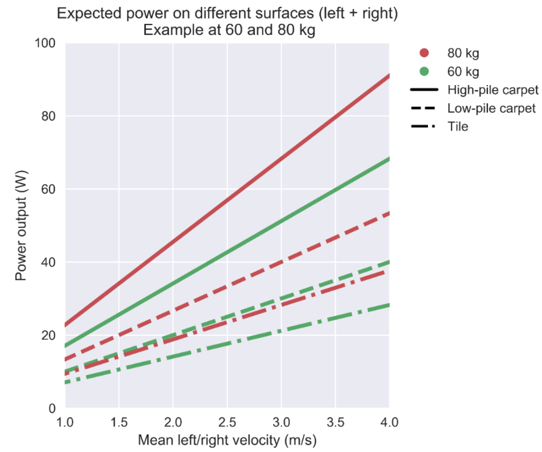

Fig. 7. Example of rolling friction simulation effect on expected power output. Friction coefficients taken from Van der Woude et al. [39] for High-pile carpet ($\mu = 0.028$), Low-pile carpet($\mu = 0.20$), and Tile ($\mu = 0.15$).

equal to 0.021 kgm^2 based on the CAD model of the roller, this was later corroborated through empirical testing (Fig. 6). Likewise, the moment of inertia of the wheelchair wheel should be considered which adds approximately 0.004 kgm^2 to the system based on an assumed gear ratio of 1.0:5.3 (roller:wheel) and a moment of inertia of 0.117 kgm^2 [25]. As such, a compensation factor on the force signal for the combined system and wheel inertia (0.025 kgm^2) was included in the control loop.

IV. Simulation Principles

The speed of the rollers is controlled by the servomotors. To calculate the speed at which the rollers should turn (v_{model}) the user generated effective force components (F_{user}) and simulated frictional components of wheelchair propulsion have to be considered together with the simulated mass for each side of the ergometer. The frictional components during wheelchair propulsion consist of the rolling resistance (F_{rr}), air resistance (F_{air}), and gravity when on a slope (F_{angle}). The resulting force (F_{res}) on one side of the wheelchair can then be calculated with (2):

$$F_{res} = F_{user} - \frac{F_{rr} - F_{air} - F_{angle}}{2} \tag{2}$$

The frictional forces are calculated separately for each wheel to allow both rollers to function independently of each other. With Newton's second law [26] we can then derive the equation of motion, given the combined mass of the wheelchair-user system (m_{tot}):

$$F_{res} = \frac{m_{tot}}{2} * a \tag{3}$$

where a is the acceleration of the wheelchair-user combination. Mass is divided by two to simulate both wheels independently. The rotational inertia of the wheels is not included. From this equation we can derive the acceleration of the wheelchair:

$$a = \frac{2 * F_{res}}{m_{tot}} \tag{4}$$

To compute the momentary speed of the wheelchair (v_{model}) for the motor controllers the acceleration is integrated:

$$v_{model} = \int a\,dt \tag{5}$$

The force on the wheelchair as a result of rolling resistance (Fig. 7) can be modelled as a simple static friction that depends on the mass of the participant and the wheelchair combined multiplied by the rolling resistance coefficient (μ), the gravitational constant (g), and adjusted for inclination (α):

$$F_{rr} = m_{tot} * g * \mu * cos(\alpha) \tag{6}$$

Air drag is a velocity dependent friction and at high speeds it becomes the most important source of friction. It is influenced by the velocity of the wheelchair (V_{wc}) and wind (V_w), the frontal plane area of the wheelchair user combination (A), the air density (D), and the aerodynamic drag coefficient (C_d):

$$F_{air} = 0.5 * D\,(V_{wc} - V_w)^2\,AC_d \tag{7}$$

Finally, when the wheelchair is going up or down a slope (α) there will be a force acting on the system as a result of gravity, this is expressed in (8):

$$F_{angle} = m_{tot} * g * sin(\alpha) \tag{8}$$

The advantage of using servomotors is that they can simulate realistic slope conditions (with exception of actual tilting of the wheelchair-user combination) where the wheelchair accelerates or decelerates accordingly, which is not possible with a braked or passive system.

Coast-down results demonstrating the simulation for a single participant in a regular handrim wheelchair are shown in Fig. 8.

V. Measurement Modes

The ergometer currently supports four different ways to evaluate wheelchair propulsion performance:

(a) *Isoinertial*
(b) *Isokinetic*
(c) *Isospeed*
(d) *Isometric*

TABLE I

COMMON OUTCOME PARAMETERS THAT CAN BE CALCULATED WITH ONLY EFFECTIVE FORCE, SPEED, AND THEIR DERIVATIVES [21]

Variable	Description	Equation
Spatio-temporal		
Push time (s)	Time from the start of positive torque to the end of positive torque for a push	$t_{end}(i)$-$t_{start}(i)$
Cycle time (s)	Time from the start of one push till the start of the next push	$t_{start}(i+1)$-$t_{start}(i)$
Push frequency (pushes/min)	Amount of pushes per minute	n_{pushes}/min
Contact angle (deg)	Amount of the handrim used per push	φ_{end}-φ_{start}
Kinetic		
Mean torque (Nm)	The mean torque (during an individual push)	$Mean_{start;end}(T)$
Peak torque (Nm)	The maximum torque (during an individual push)	$Max_{start:end}(T)$
Mean power (W)	Mean power (during the push phase)	$Mean_{start;end}(\omega*T)$
Smoothness (%)	Mean relative to the peak of push torque	Mean /Peak*100
Slope (Nm/s)	Peak toque divided by the time it takes to achieve peak torque	Peak/$t_{start:peak}$

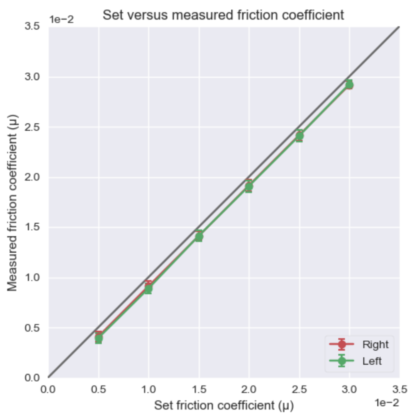

Fig. 8. Comparison between set friction in the ergometer software and friction as determined by a coast-down test with a single wheelchair-user combination. Mean and standard deviations of five trials with five separate calibrations.

The *isoinertial* mode allows for the realistic simulation of wheelchair propulsion with the previously described simulation model. It allows for the study of wheelchair biomechanics in realistic circumstances, but higher or lower (than overground) values for friction or inertia can also be used for specific research designs. Friction can be adjusted during a test or in a predefined protocol.

The *isokinetic* mode allows for realistic propulsion up to a set speed which acts like a ceiling. Participants can push the ergometer to this ceiling, but the motors will prevent going beyond that speed. In wheelchair propulsion this mode is still unexplored, but it could for example be used for max-testing.

This is similar to the *isospeed* mode in which the wheels turn at a constant speed that is not affected by external forces, which, for example, could allow for the study of speed-force relations in wheelchair propulsion. Additional safety precautions are strongly advised for this mode.

Finally, the *isometric* mode locks the breaks so a maximum force isometric strength test can be performed. This could be used to scale friction for sprint testing to the personal needs of the participant [27], [28].

VI. PROCESSING DATA

Data can be exported from LEM to a Microsoft Excel file. When exported, one can use their own algorithms to extract meaningful variables. As only the effective force can be measured, the outcome measures that can be computed are more limited than with an instrumented wheel (e.g Table I). Examples of often used outcome variables are given below. Data should first be filtered before performing further calculations [19]. The ground frequency of the measurement system is approximately 19Hz. Moreover, irregularities in the rollers and wheelchair tyres, and changes in posture all add noise to the measurement signal. As such, data in the next section were first filtered in Python (Python Software Foundation, https://www.python.org) with a 10 Hz cut-off 8th order Butterworth filter was used for the force data and a 5 Hz cut-off 4th order Butterworth filter was used on the velocity data [29]. Software for the analysis of ergometer and measurement wheels is available at [30].

VII. PRELIMINARY RESULTS

To assess the measurement capabilities of the ergometer an initial comparison was made between the ergometer and an existing commercially-available Optipush (Max Mobility, Antioch, TN, USA) measurement wheel. The measurement wheel was used as a gold standard as it has a low error [31], obtains similar results as other measurement wheels [21], and can directly measure force on the handrim, whereas the ergometer measures force more indirectly. The study was approved by the internal ethical committee (Ethische Commissie Bewegingswetenschappen). Nineteen trained able-bodied participants provided written informed-consent. They performed three blocks of four-minutes of submaximal wheelchair propulsion on the ergometer at 1.11 ms^{-1} (Fig. 2) with friction standardized to the results of an overground coast-down test in a smooth hospital hallway. The last minute of each block was used for analysis, assuming steady state propulsion.

The results are shown in Table II and fig. 9. As expected, the ergometer signal is significantly noisier than the measurement wheel data. Spatio-temporal parameters (i.e. push time, cycle time, contact angle) all showed excellent agreement (Fig. 10). However, mean power, torque, and torque per push all had excellent agreement with a moderate-excellent confidence interval and mean power per push showed an excellent agreement with a good-excellent confidence interval. Peak torques per push were higher for the ergometer and showed excellent agreement with the measurement wheel,

TABLE II

COMPARISON BETWEEN ERGOMETER AND MEASUREMENT WHEEL OUTCOME PARAMETERS DURING STEADY-STATE PROPULSION ($n = 19$)

Variable	Measurement wheel + (sd)	Ergometer value + (sd)	Difference + (%)	Absolute difference + (%)	Root mean square difference	Intraclass correlation coefficient (95% CI)[a]
Push time	0.32 (0.07)	0.32 (0.07)	0.00 (-0.07)	0.01 (2.96)	0.01	0.99 (0.97-0.99)
Cycle time	1.29 (0.54)	1.29 (0.54)	0.00 (-0.32)	0.00 (0.32)	0.01	1.00 (1.00-1.00)
Push angle	66.59 (14.17)	66.24 (13.84)	-0.35 (-0.52)	2.00 (3.00)	2.43	0.98 (0.96-0.99)
Mean torque	1.15 (0.30)	1.28 (0.27)	0.13 (11.18)	0.15 (13.41)	0.18	0.91 (0.53-0.97)
Mean power	4.24 (1.11)	4.68 (1.00)	0.45 (10.53)	0.55 (12.98)	0.64	0.92 (0.61-0.97)
Mean torque p.p	4.82 (1.30)	5.06 (1.41)	0.24 (4.98)	0.24 (4.98)	0.30	0.98 (0.62-0.99)
Peak torque p.p	8.33 (2.64)	9.08 (2.86)	2.39 (7.70)	2.39 (7.70)	2.88	0.95 (0.17-0.99)
Mean power p.p	17.78 (4.78)	18.52 (5.13)	0.74 (4.17)	0.74 (4.17)	0.97	0.98 (0.76-1.00)
Peak power p.p	31.06 (10.01)	33.46 (10.74)	2.39 (7.70)	2.39 (7.70)	2.88	0.96 (0.34-0.96)
Slope	61.88 (33.51)	79.57 (47.94)	17.68 (28.59)	17.69 (28.59)	24.05	0.84 (0.21-0.95)

a. Two-way, mixed effect, single rater, absolute agreement; p.p = per push; sd = standard deviation

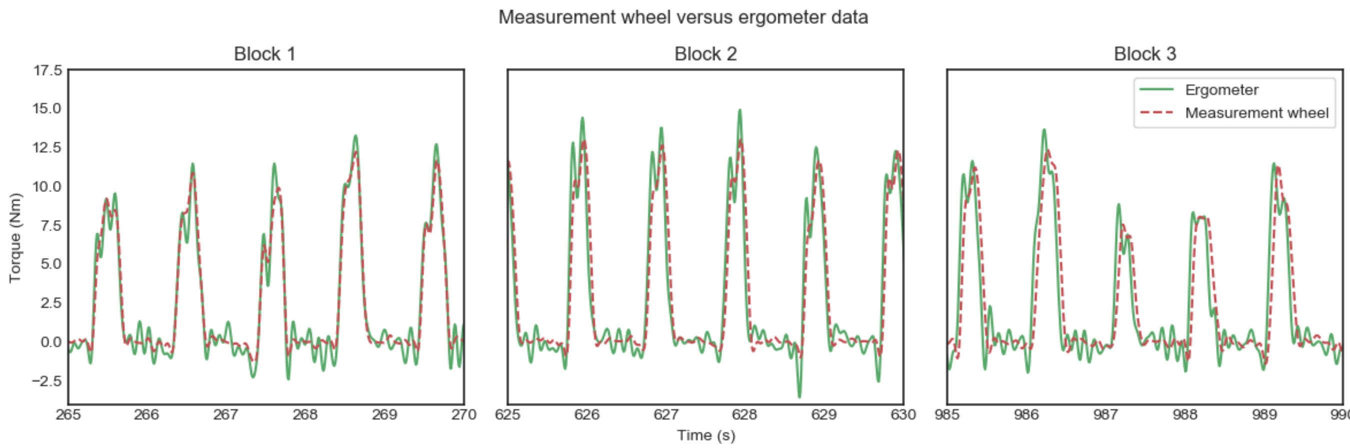

Fig. 9. Comparison of measurement wheel and ergometer data. Both signals are low-pass filtered with a 10Hz 8[th] order Butterworth filter. Typical individual example is for the last five seconds of each four-minute block for the participant with the median cycle time.

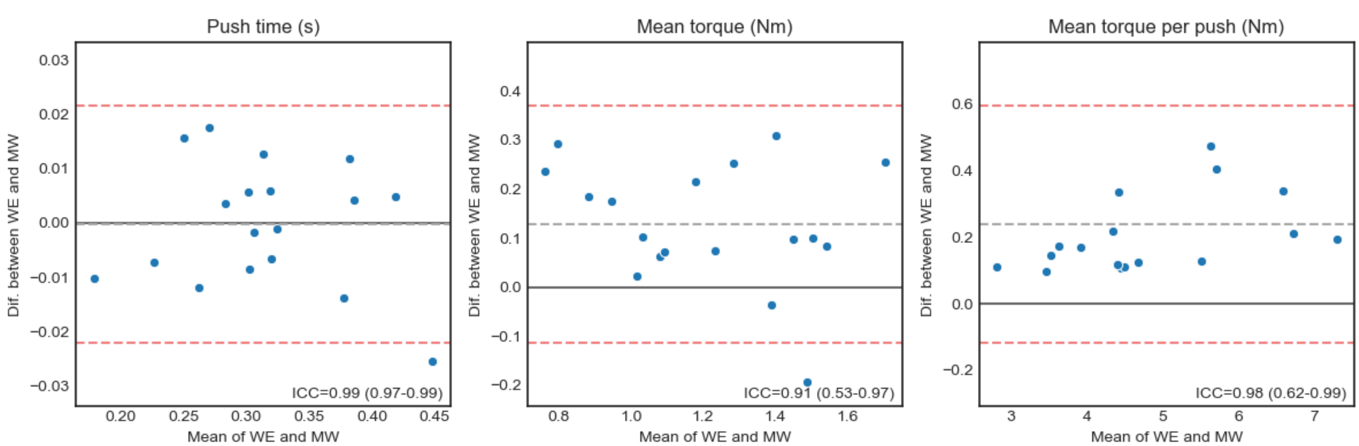

Fig. 10. Bland-Altman plots for a spatio-temporal, kinetic, and push-by-push parameter. Intraclass correlations with 95% confidence intervals are included in the right bottom of the figure. The ergometer slightly overestimates torque.

however, the confidence interval ranged from poor-excellent. Slope showed good agreement, but the confidence interval ranged from poor-excellent.

VIII. DISCUSSION

The current system can provide an appropriate simulation of overground wheelchair propulsion across a large range of frictional settings and speeds. In addition to this, it allows for push-by-push analysis of wheelchair kinetics and temporal characteristics through indirect force measurements.

The results of the coast-down tests show that, while consistent over multiple trials/calibrations, the simulated friction of the ergometer is slightly lower than expected based on the input settings of the model. This could be due to sensor drift or due to slight changes in posture of the participant. Another possibility could be that some factors that were not calibrated for influence the force readings of the ergometer and thereby the simulation. The current calibration implementation of the ergometer includes static and viscous frictional components. However, second order (or higher) frictional components are not included. Moreover, the inertia compensation is fixed and might not be appropriate for all wheelchair wheels (especially measurement wheels). In this regard, a calibration based on ramp or sinusoidal input could provide information on the nonlinear properties of the wheelchair-ergometer combination [23].

The comparison between the ergometer and the measurement wheel showed similar results and good-excellent agreement for most outcome parameters. The ergometer appears to slightly overestimate the force/torque production of the participants. More detailed calibrations with reference weights should determine the origin of this difference. Moreover, further studies using a wider range of speeds and loads should be performed to provide a broader picture of measurement accuracy. The noise could be reduced by improving the balance of the rollers, using better wheelchair wheels and construction, and investigating the effect of adjustments by the motor controller on the measurement signal.

Another difference between the ergometer and a measurement wheel is that roller ergometers by definition cannot measure handrim propulsion force. Instead, they measure the effect of the combined hand torques and propulsion force, which is pooled into one component: the effective-force component. While most wheelchair biomechanics propulsion outcomes do not require detailed (3D) information (Table I), it is essential for modelling segmental torques like in the Delft Shoulder and Elbow Model [32].

Nevertheless, the advantage of using the ergometer instead of the measurement wheels apparent [1]. The ergometer can be used with any wheelchair configuration without changing the wheelchair-user interface. This allows for faster testing, which is especially important in a clinical/sports environment. It also makes the ergometer more suitable for measuring in a sports environment as measurement wheels are usually not built for sports wheelchairs and the high strains experienced during testing of athletes [33]. Finally, the ergometer allows for the testing of different wheelchair configurations (e.g. handrim types), whereas in most measurement wheels the configuration is fixed.

The ergometer in this paper uses a simple mechanical model to simulate wheelchair propulsion. It assumes straight-line propulsion, that the wheels do not slip on the floor, the movements of the subject do not influence the wheelchair, and that the castors do not contribute to the dynamics of the wheelchair [34]. Very detailed models of wheelchair propulsion include several wheelchair parts and the centre of mass [35], [36]. However, it is not feasible to include kinematic information of body segments in a model that also directly controls the ergometer without impacting the ease-of-use. There are also models specifically built for simulating curvilinear propulsion [34], however, the majority of ergometer-based testing is on straight-line propulsion and the accuracy increase is only within the range of a few percent. The difference is between models is more pronounced for the inner wheel than for the outer wheel. Resultingly, when turning movements are of interest (e.g. for simulating tight spaces) a curvilinear model should be adopted.

The ergometer will be improved by collaborating with various research institutes, rehabilitation centres, and sports organizations. In our future work with the system the measurement performance of the ergometer will be tested with reference weights during static and dynamic conditions. For widespread adoption, standardized protocols for use in all application areas will have to be designed and validated together with researchers and clinicians. As wheelchair users form a very heterogeneous group ranging from people that seldomly propel the wheelchair themselves to Paralympic athletes with a variety of different impairments [4], it is important that the ergometer can facilitate a wide range of users, wheelchairs, and protocols.

The ergometer facilitates researchers by providing access to raw data through LEM. Moreover, the ergometer can be used in rehabilitation centres to allow for the training and assessment of patients. In this case, submaximal exercise at low loads will be more common than in research or sports settings. Practitioners should be able to quickly identify inefficient propulsion patterns (i.e. high push frequency, low contact angle [37]) and have patients adjust where necessary. In contrast to researchers, they are less interested in the raw data and they want LEM to provide the analysis for them. In the future, efficient propulsion techniques might be promoted with the use of exergames or different forms of (visual) biofeedback. Having an API available could aid in this process. Finally, in athlete assessment and training the athletes and their coaches need reliable data to monitor the status of the exercise capacity and performance ability of the athlete. The system needs to be able to withstand the high forces that a wheelchair athlete can exert on the ergometer during peak or sprint testing. Athletes also need to be able to train with standardized protocols. Again, the ergometer should provide quickly interpretable data and standardized protocols for this group of users based on input from researchers.

IX. Conclusion

The current wheelchair ergometer is able to measure and simulate wheelchair propulsion. It is presently being used for different experiments. At first, these are related to the validation of the ergometer and associated measurement protocols. Then, for studying both the physiology and biomechanics of wheelchair propulsion from early rehabilitation to sports. A variety of use-cases were presented in this paper. Our preliminary results demonstrate the functionality of the ergometer. Future research should focus on reducing the signal noise and producing standardized protocols with easy to interpret input and output.

Acknowledgment

The authors would like to thank the people at Lode BV and Umaco BV for their ongoing collaboration, sharing information, and for providing the specifications of the ergometer.

References

[1] S. van Drongelen *et al.*, "Upper extremity musculoskeletal pain during and after rehabilitation in wheelchair-using persons with a spinal cord injury," *Spinal Cord*, vol. 44, no. 3, pp. 152–159, Mar. 2006.

[2] M. Dalyan, D. Cardenas, and B. Gerard, "Upper extremity pain after spinal cord injury," *Spinal Cord*, vol. 37, no. 3, pp. 191–195, Mar. 1999.

[3] A. Rauch, SwiSCI Study Group, T. Hinrichs, C. Oberhauser, and A. Cieza, "Do people with spinal cord injury meet the WHO recommendations on physical activity?" *Int. J. Public Health*, vol. 61, no. 1, pp. 17–27, Jan. 2016.

[4] L. H. V. van der Woude, H. E. J. Veeger, A. J. Dallmeijer, T. W. J. Janssen, and L. A. Rozendaal, "Biomechanics and physiology in active manual wheelchair propulsion," *Med. Eng. Phys.*, vol. 23, no. 10, pp. 713–733, Dec. 2001.

[5] S. De Groot, R. J. K. Vegter, and L. H. V. van der Woude, "Effect of wheelchair mass, tire type and tire pressure on physical strain and wheelchair propulsion technique," *Med. Eng. Phys.*, vol. 35, no. 10, pp. 1476–1482, Oct. 2013.

[6] A. Symonds, G. Barbareschi, S. Taylor, and C. Holloway, "A systematic review: The influence of real time feedback on wheelchair propulsion biomechanics," *Disab. Rehabil., Assistive Technol.*, vol. 13, no. 1, pp. 47–53, Jan. 2018.

[7] C. Perret, "Elite-adapted wheelchair sports performance: A systematic review," *Disab. Rehabil.*, vol. 39, no. 2, pp. 164–172, Jan. 2017.

[8] R. Niesing *et al.*, "Computer-controlled wheelchair ergometer," *Med. Biol. Eng. Comput.*, vol. 28, no. 4, pp. 329–338, Jul. 1990.

[9] L. H. V. van der Woude, D.-J. E. J. Veeger, and R. H. Rozendal, "Ergonomics of wheelchair design: A prerequisite for optimum wheeling conditions," *Adapted Phys. Activity Quart.*, vol. 6, no. 2, pp. 109–132, 1989.

[10] G. J. van I. Schenau, "Some fundamental aspects of the biomechanics of overground versus treadmill locomotion," *Med. Sci. Sports Exerc.*, vol. 12, no. 4, pp. 257–261, 1980.

[11] R. de Klerk *et al.*, "Practice-based skill acquisition of pushrim-activated power-assisted wheelchair propulsion versus regular handrim propulsion in novices," *J. Neuroeng. Rehabil.*, vol. 15, no. 1, p. 56, 2018.

[12] P. L. Coe, "Aerodynamic characteristics of wheelchairs," Sci. Tech. Inf. Branch, Nat. Aeronaut. Space Admin., Washington, DC, USA, Tech. Rep. 197980191, 1979.

[13] B. Hedrick, Y. T. Wang, M. Moeinzadeh, and M. Adrian, "Aerodynamic positioning and performance in wheelchair racing," *Adapted Phys. Activity Quart.*, vol. 7, no. 1, pp. 41–51, Jan. 1990.

[14] L. van der Woude *et al.*, "Wheelchair ergonomics and physiological testing of prototypes," *Ergonomics*, vol. 29, no. 12, pp. 1561–1573, Dec. 1986.

[15] K. Bennedik, P. Engel, and G. Hildebrandt, *Der Rollstuhl: Experimentelle Grundlagen Zur Technischen Und Ergometrischen Beurteilung Handbetriebener Krankenfahrzeuge*. Heidelberg, Germany: Schindele, 1978.

[16] V. Goosey-Tolfrey, "BASES physiological testing guidelines: The disabled athlete," *Sport Exerc. Physiol. Test. Guidelines*, vol. 1, p. 10, 2007.

[17] B. Mason, J. Lenton, C. Leicht, and V. Goosey-Tolfrey, "A physiological and biomechanical comparison of over-ground, treadmill and ergometer wheelchair propulsion," *J. Sports Sci.*, vol. 32, no. 1, pp. 78–91, Jan. 2014.

[18] R. de Klerk *et al.*, "Measuring handrim wheelchair propulsion in the lab: A critical analysis of stationary ergometers," *IEEE Rev. Biomed. Eng.*, vol. 13, pp. 199–211, 2020.

[19] R. A. Cooper, "Frequency analysis of 3-dimensional pushrim forces and moments for manual wheelchair propulsion," *Automedica*, vol. 16, pp. 355–365, 1998.

[20] H. E. Veeger, L. H. van der Woude, and R. H. Rozendal, "A computerized wheelchair ergometer. Results of a comparison study," *Scand. J. Rehabil. Med.*, vol. 24, no. 1, pp. 17–23, 1992.

[21] R. J. Vegter, C. J. Lamoth, S. de Groot, D. H. Veeger, and L. H. van der woude, "Variability in bimanual wheelchair propulsion: Consistency of two instrumented wheels during handrim wheelchair propulsion on a motor driven treadmill," *J. NeuroEng. Rehabil.*, vol. 10, no. 1, p. 9, 2013.

[22] S. Groot *et al.*, "WHEEL-I: Development of a wheelchair propulsion laboratory for rehabilitation," *J. Rehabil. Med.*, vol. 46, no. 6, pp. 493–503, 2014.

[23] C. P. DiGiovine, R. A. Cooper, and M. L. Boninger, "Dynamic calibration of a wheelchair dynamometer," *J. Rehabil. Res. Develop.*, vol. 38, no. 1, pp. 41–55, Jan./Feb. 2001.

[24] P. Virtanen *et al.*, "SciPy 1.0: Fundamental algorithms for scientific computing in Python," *Nature Methods*, 2020. [Online]. Available: https://rdcu.be/b08Wh, doi: 10.1038/s41592-019-0686-2.

[25] S. Sprigle, M. Huang, and J.-T. Lin, "Inertial and frictional influences of instrumented wheelchair wheels," *J. Rehabil. Assistive Technol. Eng.*, vol. 3, Jun. 2016, Art. no. 205566831664989.

[26] I. Newton, *Mathematical Principles of Natural Philosophy*. London, U.K.: A. Strahan, 1802.

[27] J. van der Scheer, S. de Groot, R. J. K. Vegter, D. Veeger, and L. H. V. van der Woude, "Can a 15 m-overground wheelchair sprint be used to assess wheelchair-specific anaerobic work capacity?" *Med. Eng. Phys.*, vol. 36, no. 4, pp. 432–438, Apr. 2014.

[28] T. W. J. Janssen, C. A. J. M. van Oers, A. P. Hollander, H. E. Veeger, and L. H. V. van der Woude, "Isometric strength, sprint power, and aerobic power in individuals with a spinal cord injury," *Med. Sci. Sports Exerc.*, vol. 25, no. 7, pp. 863–870, Jul. 1993.

[29] S. de Groot, F. Bos, J. Koopman, A. E. Hoekstra, and R. J. K. Vegter, "The effect of a novel square-profile hand rim on propulsion technique of wheelchair tennis players," *Appl. Ergonom.*, vol. 71, pp. 38–44, Sep. 2018.

[30] R. de Klerk, "Worklab: A wheelchair biomechanics mini-package (version 1.0.0)," Zenodo, Univ. Med. Center Groningen, Univ. Groningen, Groningen, The Netherlands, Jul. 2019, doi: 10.5281/zenodo.3268671.

[31] L. Guo, A. M. Kwarciak, R. Rodriguez, N. Sarkar, and W. M. Richter, "Validation of a biofeedback system for wheelchair propulsion training," *Rehabil. Res. Pract.*, vol. 2011, Oct. 2011, Art. no. 590780.

[32] A. A. Nikooyan, H. E. J. Veeger, E. K. J. Chadwick, M. Praagman, and F. C. T. Van Der Helm, "Development of a comprehensive musculoskeletal model of the shoulder and elbow," *Med. Biol. Eng. Comput.*, vol. 49, no. 12, pp. 1425–1435, Dec. 2011.

[33] V. L. Goosey-Tolfrey, N. E. Fowler, I. G. Campbell, and S. D. Iwnicki, "A kinetic analysis of trained wheelchair racers during two speeds of propulsion," *Med. Eng. Phys.*, vol. 23, no. 4, pp. 259–266, May 2001.

[34] F. Chénier, P. Bigras, and R. Aissaoui, "A new dynamic model of the wheelchair propulsion on straight and curvilinear level-ground paths," *Comput. Methods Biomech. Biomed. Eng.*, vol. 18, no. 10, pp. 1031–1043, Jul. 2015.

[35] J. Bascou, C. Sauret, H. Pillet, P. Vaslin, P. Thoreux, and F. Lavaste, "A method for the field assessment of rolling resistance properties of manual wheelchairs," *Comput. Methods Biomech. Biomed. Eng.*, vol. 16, no. 4, pp. 381–391, Apr. 2013.

[36] M. Hofstad and P. E. Patterson, "Modelling the propulsion characteristic of a standard wheelchair," *J. Rehabil. Res. Develop.*, vol. 31, no. 2, pp. 129–137, 1994.

[37] B. Sawatzky, C. Digiovine, T. Berner, T. Roesler, and L. Katte, "The need for updated clinical practice guidelines for preservation of upper extremities in manual wheelchair users: A position paper," *Amer. J. Phys. Med. Rehabil.*, vol. 94, no. 4, pp. 313–324, Apr. 2015.

[38] F. Chenier, P. Bigras, and R. Aissaoui, "A new wheelchair ergometer designed as an admittance-controlled haptic robot," *IEEE/ASME Trans. Mechatronics*, vol. 19, no. 1, pp. 321–328, Feb. 2014.

[39] L. van der woude, C. Geurts, H. Winkelman, and H. Veeger, "Measurement of wheelchair rolling resistance with a handle bar push technique," *J. Med. Eng. Technol.*, vol. 27, no. 6, pp. 249–258, Jan. 2003.